On the links between ice nucleation, cloud phase, and climate sensitivity in CESM2

Zachary McGraw[1,2*], Trude Storelvmo[3], Lorenzo Polvani[1,4,5], Stefan Hofer[3], Jonah Shaw[6,7], Andrew Gettelman[8,‡]

1 Department of Applied Physics and Applied Mathematics, Columbia University, New York, NY, USA
2 NASA Goddard Institute for Space Studies, New York, NY, USA
3 Department of Geosciences, University of Oslo, Oslo, Norway
4 Department of Earth and Environmental Sciences, Columbia University, New York, NY, USA
5 Lamont-Doherty Earth Observatory, Columbia University, Palisades, NY, USA
6 Department of Atmospheric and Oceanic Sciences, University of Colorado Boulder, Boulder, CO, USA
7 Cooperative Institute for Research in Environmental Sciences, University of Colorado Boulder, Boulder, CO, USA
8 National Center for Atmospheric Research, Boulder, Colorado
‡ Now at Pacific Northwest National Laboratory, Richland, WA, USA

* corresponding author: zachary.mcgraw@columbia.edu

Mixed-phase clouds greatly affect projections of future climate, with recent evaluations highlighting the influence of the ice nucleation process in these clouds. Here we explore how this process affects climate sensitivity using simulations of the Community Earth System Model version 2 (CESM2). Ice nucleation is found to influence simulated cloud feedbacks not just over extratropical low clouds but over most regions and levels of the troposphere. However, the otherwise major influence of ice nucleation on total cloud feedback is negated when holding global mean cloud phase to observed levels. In satellite-constrained model experiments, dissimilar ice nucleation realizations all result in a strongly positive total cloud feedback, as in the default model. Global-scale cloud phase is hence confirmed to be the dominant link between ice nucleation and climate sensitivity. Conversely, whether ice nucleation is treated as aerosol-sensitive is found to be of limited importance. A microphysics update from CESM1 to CESM2 had substantially weakened ice nucleation in mixed-phase clouds, in part due to a model issue. Our findings suggest that this contributed to increased climate sensitivity primarily by reducing a global-scale cloud phase bias. Despite the issue, CESM2's ice nucleation appears to form more realistic mixed-phase clouds than either a corrected implementation or CESM1's ice nucleation scheme.

Key points

- Simulated relationships among ice nucleation, cloud phase, and feedback strength are largely set by mid-level and tropical high clouds.
- Ice nucleation has only weak influence on simulated total cloud feedback when global mean cloud phase is maintained at observed levels.
- CESM2's strongly positive cloud feedback is consistent with realistic mixed-phase cloud representation despite a known model issue.

Introduction

Mixed-phase clouds are a key source of uncertainty in projections of future climate (Forster et al., 2021; Storelvmo et al., 2015), yet their influence is poorly understood or constrained. These clouds exist at temperatures where either liquid droplets or ice crystals may form (roughly -38°C to 0°C) and are governed by microphysical interactions between water's three thermodynamic phases (vapor, liquid, and ice) (Korolev et al., 2017). The importance of these processes has been brought to light by a number of studies (Frey & Kay, 2018; Tan & Storelvmo, 2016; Zhu et al., 2022) that uncovered major changes to projected climate after altering mixed-phase clouds in global simulations. Most critically, these studies reported strong impacts on the global mean surface air temperature change that ultimately develops following a doubling of carbon dioxide in the atmosphere, a central metric in climate science known as *equilibrium climate sensitivity* (ECS).

The established link between mixed-phase clouds and ECS is the *cloud phase feedback* (Mitchell et al., 1989), wherein warming ice clouds slow global climate change by deglaciating into liquid clouds. Since cloud droplets tend to be smaller than ice crystals, deglaciation results in more exposed surface area per unit mass (i.e. optically thicker clouds), hence more reflection of sunlight and lower ECS. This negative feedback has been most associated with near-surface clouds at high latitudes, especially over the Southern Ocean. Climate model estimates of ECS have been found to overestimate this feedback, implying underestimated global warming (Tan et al., 2016). This is linked to a deficiency of cloud liquid relative to total cloud condensate (*supercooled liquid fraction*, or SLF) in these models compared to satellite retrievals (Komurcu et al., 2014), leaving simulated clouds with excessive ability to deglaciate with warming. Effort to correct this bias has been proposed as a major reason that an unprecedented proportion of contemporary climate models have high climate sensitivity (>4.5°C) (Zelinka et al., 2020).

Multiple realizations of microphysical processes may result in similar global mean SLF (Tan et al., 2016). It is unknown which microphysical processes most account for the present-day proportion of ice, and to what degree each process will affect ECS by responding to warming. In mixed-phase clouds, ice may be locally formed through freezing of cloud droplets containing aerosol that act as *ice nucleating particles* (INPs) (Kanji et al., 2017). Alternatively, ice crystals may fall from overlying cirrus or be detrained from deep convective cores. Once ice crystals are present, these may grow by depleting surrounding liquid droplets via the Wegener-Bergeron-Findeisen (WBF) vapor deposition process (Storelvmo & Tan, 2015). Frequently, the WBF process makes ice crystals grow sufficiently heavy to initiate precipitation. The described influences of ice formation processes on cloud phase and occurrence are shown in Figure 1a.

Recent publications have highlighted the influence of ice nucleation on ECS (Gettelman et al., 2019; Murray et al., 2021; Zhu et al., 2022). Ice nucleation is a complex process that continues to evolve within climate models. Laboratory experiments have consistently found ice nucleation to act strongest in environments with abundant aerosols capable of acting as INPs (Kanji et al., 2017), yet models do

not typically make ice nucleation sensitive to aerosols (*aerosol-sensitive*). It has been argued that constraining ECS will necessitate a realistic treatment of aerosol-sensitive ice nucleation (Murray et al., 2021). Apparently supporting this hypothesis, ice nucleation developments in the Community Earth System Model (CESM) have been implicated in sizable ECS shifts. The CMIP6 version of this model (CESM2) featured updates over the earlier CESM1 that intended to make ice nucleation in the mixed-phase cloud regime aerosol-sensitive. Concurrently, simulated ECS jumped from 4.0K to 5.3K. Adding confusion, a model bug identified by authors of the present study negated much of the new ice nucleation scheme's influence (Shaw et al., 2022). Reversion to CESM1's ice nucleation scheme was found to undo most of the feedback difference causing the ECS jump (Gettelman et al., 2019), while correcting the bug considerably lowered ECS in a reduced-resolution version of CESM2 (Zhu et al., 2022). However, an update to CESM2's microphysics that replaced the ice nucleation scheme while removing the bug only weakly affected ECS (Gettelman et al., 2022). The connection between ice nucleation and ECS remains poorly understood.

Here we assess how and to what extent ice nucleation in mixed-phase clouds influences climate sensitivity. Cloud feedbacks are evaluated in CESM2 simulations with varied realizations of ice nucleation, including both aerosol-sensitive and aerosol-independent representations. A detailed analysis reveals that feedbacks in mid-level and high clouds play an outsize role in setting relationships between ice nucleation representation and feedback strength. We report little influence of ice nucleation representation on cloud feedback strength as long as simulated cloud phase is kept consistent with global-scale observations. Using knowledge from our experiments, we comment on CESM2's ice nucleation scheme and its role in this model's high climate sensitivity.

Methods

Here we perform two groups of model experiments with the CESM2 global climate model (Danabasoglu et al., 2020). The experimental setup is visualized in Fig. 1b. In the first experiments (hereafter *Group A*), we alter simulated ice nucleation only, which results in lower SLF for schemes with stronger ice nucleation. In the second (*Group B*), we alter ice nucleation while adjusting the WBF process to maintain constant global mean cloud phase at observed levels. Group A experiments allow us to assess the role of cloud phase bias in models with strong uncompensated ice nucleation, while Group B represents distinct plausible realizations of mixed-phase clouds. Except for the differences described herein, simulations are carried out with the model version used in CMIP6 at its 1.25°x0.9° resolution. Within CESM2, microphysical processes pertaining to the formation and development of stratiform mixed-phase clouds – including ice nucleation and WBF – are treated by the (Gettelman & Morrison (2015) microphysics scheme. The physical parameterizations in the atmospheric component of CESM2, the Community Atmosphere Model version 6 (CAM6) are described by (Gettelman et al., 2019). For each experiment, we ran two 10-year simulations having fixed sea surface temperatures (SSTs). One simulation has present-day climatology while the other has SSTs uniformly raised by 4°C (Cess et al., 1989). Cloud feedbacks were then evaluated using a kernel method described later in this section.

In the first set of experiments *(*Group A*)*, we tested the default model (hereafter referred to as *Default*) as well as three alternative ice nucleation realizations (listed in Table 1). In CESM2, an aerosol-sensitive ice nucleation scheme (Hoose et al., 2010) is enabled by default. However, an overlooked limit on ice number negates this ice number source to zero, reducing the Hoose scheme's influence to small ice mass sources. For our second experiment, we correct the problematic limit to avoid negating the Hoose scheme's direct impact on ice number (experiment *Hoose (A)*). We additionally test the model with all local ice nucleation terms set to zero (*No INPs (A)*). Lastly, we test the aerosol-independent strong ice nucleation source of CESM1 (Meyers et al., 1992) (hereafter *Meyers (A)*).

For the SLF-constrained experiments (Group B), ice nucleation is again altered but we negate the global impact on cloud phase. Specifically, we adjust the WBF process to bring global mean SLF within ±1°C of the -20°C isotherm to that observed by the CALIOP satellite (Tan et al., 2016). This method is based on the two SLF-constrained experiments in Tan et al., (2016), which had different INP concentrations with the same ice nucleation scheme yet similar global mean SLF. To improve SLF agreement for warmer isotherms, we also reduce the proportion of ice phase detrained from convective cores as in Tan & Storelvmo (2016), here simultaneously doubling detrained liquid radius to offset impacts on cloud radiative effects. For each experiment, the WBF process is then adjusted by a constant efficiency multiplier to keep cloud phase within the observed range (see simulated cloud phase at -20°C in Table 1, and other isotherms in Figure S2). To ensure SLF from the model and retrievals are comparable, we use custom model output that considers only the clouds observable to CALIOP, as in Komurcu et al. (2014). We repeat experiments *No INPs (A)* and *Meyers (A)* through this methodology. The *Hoose (A)* experiment reveals that the Hoose scheme with no further modification directs an overabundance of ice crystals to latitudes around major mineral dust INP sources (i.e. Saharan and Middle-Eastern deserts) compared to DARDAR-Nice satellite retrievals (Sourdeval et al., 2018) (see experiment *Hoose (A)* in Figure S1a). Since Group B experiments are intended to be plausible mixed-phase cloud representations, we here reduce this scheme's efficiency to improve ice nucleation spatial variability agreement. We simulate the Hoose scheme in two Group B experiments, having dust INPs capped to 5% and 20% of total mineral dust concentrations (*Hoose-cap1 (B)* and *Hoose-cap2 (B)*, respectively). That these experiments represent a relatively weak and strong aerosol-sensitive ice nucleation makes them the Group B equivalents of *Default* and *Hoose (A)*. Note that we do not attempt to correct for disagreement between simulated and retrieved global mean ice number. Ice number is overall lower than retrievals for both cirrus and mixed-phase cloud isotherms (see Fig. S1b), suggesting this may relate to biases in cirrus formation and sedimentation rather than ice nucleation in mixed-phase clouds.

In order to calculate total cloud feedback and its decomposition into cloud optical depth, amount, and altitude feedback mechanisms, we use a radiative kernel method (Zelinka et al., 2012a; Zelinka et al., 2012b). This kernel method estimates the radiative impact of changes across two climate states among 49 cloud categories, as shown in Figure S3. Individual mechanisms are distinguished based on patterns of cloud changes in a warmer future. The Zelinka kernel uses as input 2D cloud fractions standardized

by the International Satellite Cloud Climatology Project (ISCCP) (Rossow & Schiffer, 1999), which divides clouds into 7 cloud top pressure and 7 cloud optical depth categories. A residual term exists between the total feedback and sum of feedback mechanisms, which includes interactions among feedback mechanisms. We further separate feedbacks between those operating in low (cloud top pressure >680 hPa), mid-level (440-680 hPa), and high clouds (<440 hPa) through a refined decomposition method (Zelinka et al., 2016). Note that this partitioning of cloud feedbacks alters their attribution by mechanism, such that the sum of a feedback mechanism across all cloud levels is different than its unpartitioned magnitude. ISCCP cloud histograms were output from the model using the CFMIP Observation Simulator Package (COSP) (Bodas-Salcedo et al., 2011), then analyzed with the kernel method.

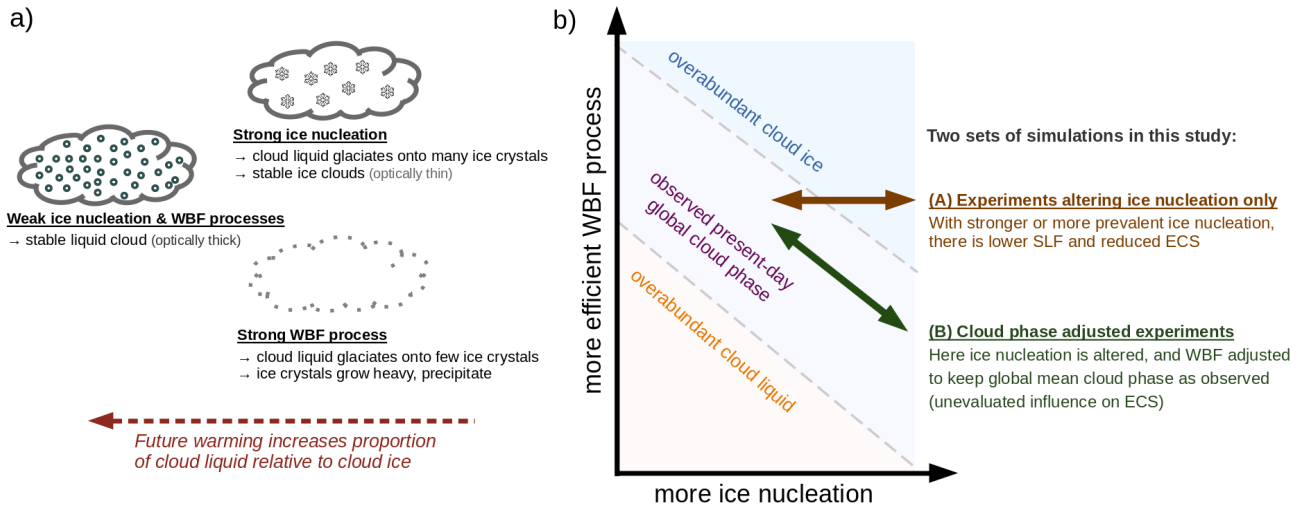

Figure 1 | Ice formation processes, their influence on cloud properties and ECS, and our experimental setup. Shown are conceptual diagrams linking microphysical processes with mixed-phase cloud properties **(a)** and climate sensitivity **(b)**. Strengthening of ice nucleation could represent either more INPs in individual locations or increased INP prevalence across locations.

Table 1 | Experimental setup and relevant cloud properties from simulations and observations of present-day climate. All values are global averages except where noted.

experiment group & name		experimental setup			Present-day cloud properties						
		Ice nucleation in mixed-phase clouds	WBF efficiency		SLF at -20°C global (%)	SLF at -20°C *40-70°S* (%)	SLF at -20°C *15°S-15°N* (%)	Cloud radiative effects shortwave (W/m^2)	Cloud radiative effects longwave (W/m^2)	Cloud ice water path (g/m^2)	Cloud liquid water path (g/m^2)
Group A *altered INPs only*	*No INPs*	none	100%		23.7	37.5	12.6	-47.9	23.9	12.7	67.5
	Default	Hoose et al 2010 *ice number sources suppressed*	100%	*more INPs*	21.6	34.6	11.5	-47.7	23.8	13.0	65.9
	Hoose	Hoose et al 2010 *corrected ice limit*	100%		14.7	26.8	9.6	-48.8	24.9	15.7	61.8
	Meyers	Meyers et al 1991	100%		4.3	8.3	1.9	-45.9	22.7	14.3	54.4
Group B *phase-constrained*	*No INPs*	none	100%		31.1	48.4	18.6	-48.7	24.3	10.8	74.5
	Hoose-cap1	Hoose et al 2010 *corrected ice limit, max 5% dust*	65%	*more INPs, weaker WBF*	28.7	49.7	19.3	-48.2	24.2	11.7	69.5
	Hoose-cap2	Hoose et al 2010 *corrected ice limit, max 20% dust*	50%		30.3	52.0	21.7	-48.9	24.7	12.8	69.4
	Meyers	Meyers et al 1991	25%		31.3	47.6	23.6	-51.2	26.1	15.3	70.0
	observations				27–32 *			-46 **	28 **	12 –140 †	15 –102 †

* *(Tan et al., 2016)*
** *(Loeb et al., 2018)*
† *(Jiang et al., 2012)*

Results

How INPs influence cloud feedback strength

In the absence of further adjustments, adding INPs reduces present-day SLF (see Group A averages in Table 1). Comparing experiments reveals a strong correlation between global mean SLF and cloud feedback strength. This is evident in Fig. 2a, where Group A simulations are represented as triangles. We here assess the mechanisms that drive this link and to what extent ice nucleation's sensitivity to aerosols influences cloud feedback strength.

Contrary to expectations, differences in cloud feedback cannot be explained merely by simulated impacts on low clouds. In fact, among our CESM2 simulations, most differences in total cloud feedback are attributable to mid-level and high clouds. This is shown in Figure 2b. Accordingly, experiments with strong ice nucleation and no compensating change (*Meyers (A)* and *Hoose (A)*, represented as red and green triangles, respectively) have the lowest total cloud feedback strengths among experiments yet unremarkable low cloud feedback strengths. One explanation is that a portion of the simulated cloud phase feedback operates in mid-level clouds. Both INPs and warming are found

to alter cloud optical depth up to pressure levels of approximately 440mb (see Figs. S4 and S6 for ISCCP cloud type histogram comparisons). Consequently, while low cloud optical depth is more negative in both *Hoose (A)* and *Meyers (A)* than in *No INPs (A)*, the especially prevalent *Meyers (A)* ice nucleation also results in a more negative mid-level cloud optical depth feedback (compare red bars in Fig. 3a). Additionally, INPs are found to enhance the positive cloud amount feedback in low clouds – negating INPs' influence on low cloud optical depth feedback – yet have an opposite impact on mid-level clouds (see blue bars in Fig. 3a). These amount feedback effects cancel when considering both cloud levels together, yet strongly enhance the attribution of cloud feedback differences to mid-level clouds. INPs enhance the simulated occurrence of low clouds yet reduce mid-level cloud occurrence (compare sums over rows in Fig. S4), affecting the potential for the amount feedback to operate at each level. This contrast may result from INP-induced precipitation having an amplified influence in vertically developed liquid clouds compared to shallow near-surface clouds. INPs can generate precipitation in clouds that are otherwise too ice-starved to undergo the WBF process, yet in other cases may prevent ice crystals from falling by distributing condensate mass among many crystals. Both INP impacts mentioned so far primarily operate over extratropical clouds (compare dashed lines in Fig. 3b, and see Fig. S8 for feedbacks divided by both latitude and mechanism).

The aerosol-sensitive *Hoose (A)* ice nucleation does not reduce low and mid-level cloud feedbacks to the extent of *Meyers (A)*, yet this difference is partly offset by a feedback in high clouds (compare red and green triangles in Fig. 2b). Though influence of mixed-phase microphysics on high cloud feedbacks has not previously been examined, the cold isotherms where ice nucleation acts strongest are typically above 440 hPa in the tropics and sub-tropics. The *Hoose (A)* experiment creates greater present-day high cloud occurrence than in any other experiment (see second to last row of Fig. S4). This is likely a result of heavily concentrated INPs around the sub-tropical dust belt, which stabilize ice cloud occurrence more than they diminish liquid cloud occurrence. This generates a regional negative cloud amount feedback (see the green dashed line in Fig. 3b, bottom row). That warming reduces these clouds more than in other experiments (compare central columns of Fig. S6) may result from these clouds precipitating out as ice nucleation weakens with warming, resulting in fewer, heavier ice crystals. This may either be a novel feedback mechanism or an issue in models having unrealistically concentrated INPs. Overall, our simulations reveal INP influence on cloud feedback strength to operate through more mechanisms and cloud types than have previously been considered. These are summarized in Table 2.

Negligible influence of INPs when controlling for cloud phase

Now we turn to the influence of ice nucleation when controlling for global cloud phase (Group B experiments). Feedback differences are noticeably more modest than Group A experiments in all cloud top pressure groupings (compare circles to triangles in Fig. 2). There are multiple reasons for this. First, none of the Group B experiments show INPs to affect mid-level cloud optical depth feedback like in the *Meyers (A)* experiment (compare red bars in Fig. 3a, third row). This suggests that ice nucleation's impacts are most pervasive when operating in tandem with a strong WBF process. Second, the WBF

adjustment to maintain global mean SLF causes a counterbalancing feedback in high clouds. In experiments with abundant INPs (*Meyers (B)* and *Hoose-cap2 (B)*), high cloud optical depth feedback is less negative than in other Group B experiments (see red bars in Fig. 3a, bottom panel). This appears to reflect that the WBF adjustment increases SLF near the equator (see in Table 1 that this is evident only in Group B experiments) to compensate for SLF decreases elsewhere (see SLFs by latitude in Fig. S2b). Differences in optical depth feedback among these experiments are thus opposite in high tropical clouds as in lower polar clouds. See Table 2 for a summary of mechanisms resulting in the balanced impact of INPs on cloud feedback strength in these experiments.

Ice nucleation's sensitivity to aerosol concentrations has only weak influence on feedback strength in these SLF-constrained experiments. A key aim for modeling this process as aerosol-sensitive is to represent impacts of Southern Ocean INP-scarcity on regional cloud phase and its associated feedback (Murray et al., 2021). Surprisingly, in our simulations this region's SLF is much higher than other regions even with no INPs (see similar values in Table 1 among *No INPs (B)* and *Hoose-cap2 (B)*). This is likely because ice crystal sources from cirrus and convective detrainment are similarly lacking in this region. As explained in Methods, strong aerosol-sensitive ice nucleation appears incompatible with satellite retrievals. Hence ice nucleation within mixed-phase clouds may be modest relative to other ice crystal sources, limiting the influence of INP representation.

Impact of ice nucleation error in CESM2

Due to the ice nucleation error in CESM2, the default model (*Default* experiment here) has a relatively modest – yet non-negligible – ice nucleation source. Consequently, the default cloud properties (see Table 1) and cloud feedbacks (see Figs. 2 & 3) are between those with no INPs (*No INPs (A)*) and with the error corrected (*Hoose (A)*). By comparison, the intended strong aerosol-sensitive ice nucleation scheme would have resulted in more heavily biased SLF (see Fig. S2a) and an above-described issue with ice number spatial variability.

We found that global-scale cloud phase is the dominant link between INPs and feedback strength, while CESM2's ice nucleation scheme reduces the cloud phase bias present with the CESM1 scheme. These results imply that, despite the error, mixed-phase cloud influence on ECS is more realistic in CESM2 than with the earlier ice nucleation treatment. In fact, all of our observation-constrained (Group B) experiments have a total cloud feedback that is even more positive than in default CESM2. Further, we find the error to only directly affect global cloud feedback strength by +0.02 $W/m^2/K$ (comparing *No INPs (A)* to *Hoose (A)*). Ice nucleation appears only capable of substantially reducing simulated ECS if represented as so strong that it generates a large bias in cloud phase. This was the case with CESM1's ice nucleation scheme (Tan et al., 2016) (*Meyers (A)* experiment here).

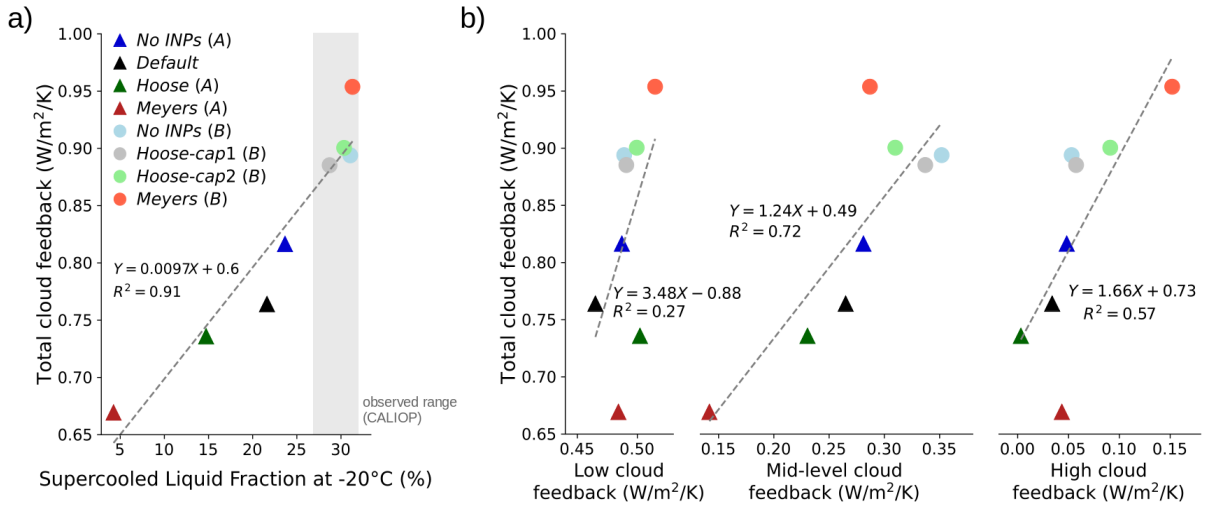

Figure 2 | Relationships among cloud phase, total cloud feedback, and feedbacks grouped by cloud top pressure. Shown is the relationship between supercooled liquid fraction (SLF) at -20 °C and cloud feedback strength **(a)**, as well as the relationships between feedbacks operating in low, mid-level, and high clouds to their total **(b)**. All values are global averages. In (a), the SLF range from CALIOP satellite retrievals is shown for comparison.

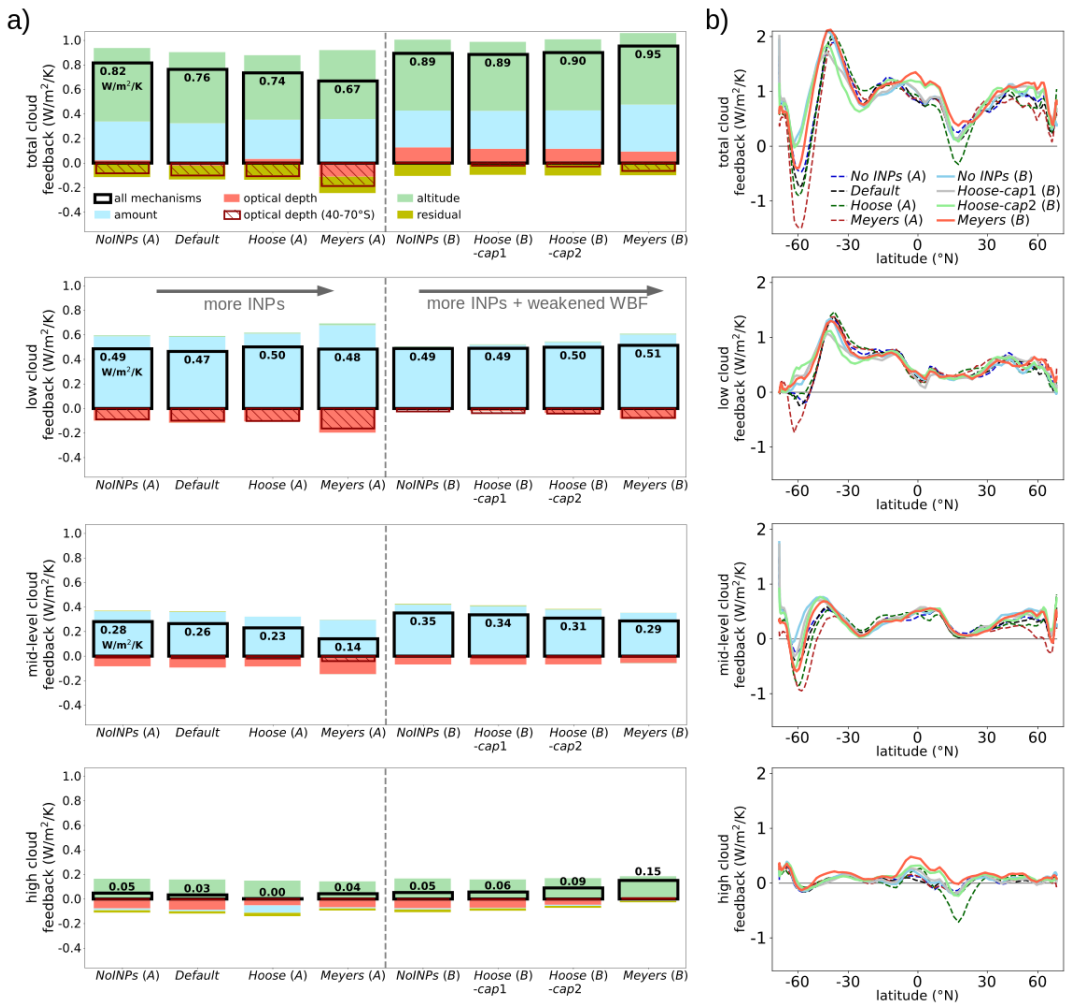

Figure 3 | Cloud feedback strength by location and mechanism, showing cloud feedbacks in all model experiments, both split by individual mechanisms **(a)** and by latitude **(b)**. All data in (a) are global means, aside for the red hatches showing contributions of optical depth feedback over 40-70°S (mean feedback over this region multiplied by its 14.8% share of global surface area). Black hollow bars show sums of all mechanisms, with values in W/m^2/K included as black text.

Table 2 | Simulated links between INPs and cloud feedbacks reported in this study

Feedback type	Cloud type	Region	Sign of feedback	Impact of increasing INPs *among unadjusted experiments (Group A)*	Impact of increasing INPs *among SLF-constrained experiments (Group B)*
optical depth	low	extratropics	-	stronger	moderately stronger
	mid-level	extratropics	-	stronger (*Meyers* nucleation only)	negligible
	high	equatorial	-	negligible/unclear	moderately weaker
amount	low	extratropics	+	stronger*	moderately stronger*
	mid-level	extratropics	+	weaker*	moderately weaker*
	high	Dust Belt region	+	moderately weaker (*Hoose* nucleation only)	negligible
total cloud feedback			+	weaker	negligible

* Differences in low and mid-level cloud amount feedback closely cancel, and hence have little influence on total cloud feedback.

Discussion

The dominant link between mixed-phase cloud microphysics and climate sensitivity in CESM2 is shown to be cloud phase, with independent differences in ice nucleation strength and variability having far less influence. Ice nucleation model treatment is found to noticeably affect simulated cloud phase feedback over the Southern Ocean, as suggested in *Murray et al 2021*. However, our CESM2 experiments reveal only weak differences in total cloud feedback strength when controlling for present-day global mean cloud phase. Note that we did not run simulations coupled to an interactive ocean model. We hence did not directly estimate ECS, which may be affected by interactions between cloud and non-cloud feedback mechanisms (Lohmann & Neubauer, 2018).

Our findings suggest that CESM2's ice nucleation updates raised ECS primarily by correcting – partially inadvertently – much of the cloud phase bias present in CESM1 (Tan et al., 2016). Our findings are consistent with results from a new version of CESM2's microphysics with revised ice nucleation (Gettelman et al., 2022), which did not lead to substantial change in ECS. Correcting the ice limit issue in a reduced-resolution CESM2 version had reduced cloud feedback strength (Zhu et al., 2022), yet we find this does not occur in the standard-resolution model. In fact, our observationally-constrained simulations produced higher total cloud feedback than default CESM2 regardless of ice nucleation scheme. A caveat is that CESM2's ECS is already stronger than evidence suggests is likely (Sherwood et al., 2020), which may relate to biases in other cloud types.

A key result of this study is that microphysical processes in mixed-phase clouds influence climate sensitivity not just through low cloud optical depth feedback, but through mechanisms operating wherever clouds exist in the relevant temperature range. Mid-level and high clouds are found to largely drive the global influence of INPs on cloud feedback strength, yet controlling for cloud phase alters these clouds in ways that negate this influence. Future research should assess whether these mechanisms are robust or are model artifacts that problematically influence climate projections.

Bodas-Salcedo, A., Webb, M. J., Bony, S., Chepfer, H., Dufresne, J.-L., Klein, S. A., Zhang, Y., Marchand, R., Haynes, J. M., Pincus, R., & John, V. O. (2011). COSP: Satellite simulation software for model assessment. *Bulletin of the American Meteorological Society*, *92*(8), 1023–1043. https://doi.org/10.1175/2011BAMS2856.1

Cess, R. D., Potter, G. L., Blanchet, J. P., Boer, G. J., Ghan, S. J., Kiehl, J. T., Le Treut, H., Li, Z.-X., Liang, X.-Z., Mitchell, J. F. B., Morcrette, J.-J., Randall, D. A., Riches, M. R., Roeckner, E., Schlese, U., Slingo, A., Taylor, K. E., Washington, W. M., Wetherald, R. T., & Yagai, I. (1989). Interpretation of Cloud-Climate Feedback as Produced by 14 Atmospheric General Circulation Models. *Science*, *245*(4917), 513–516.

Danabasoglu, G., Lamarque, J.-F., Bacmeister, J., Bailey, D. A., DuVivier, A. K., Edwards, J., Emmons, L. K., Fasullo, J., Garcia, R., Gettelman, A., Hannay, C., Holland, M. M., Large, W. G., Lauritzen, P. H., Lawrence, D. M., Lenaerts, J. T. M., Lindsay, K., Lipscomb, W. H., Mills, M. J., … Strand, W. G. (2020). The Community Earth System Model Version 2 (CESM2). *Journal of Advances in Modeling Earth Systems*, *12*(2), e2019MS001916. https://doi.org/10.1029/2019MS001916

Forster et al. (2021). *Chapter 7: The Earth's Energy Budget, Climate Feedbacks and Climate Sensitivity* (Climate Change 2021: The Physical Science Basis. Contribution of Working Group I to the Sixth Assessment Report of the Intergovernmental Panel on Climate Change.). Cambridge University Press. https://doi.org/10.1017/9781009157896.009

Frey, W. R., & Kay, J. E. (2018). The influence of extratropical cloud phase and amount feedbacks on climate sensitivity. *Climate Dynamics*, *50*(7), 3097–3116. https://doi.org/10.1007/s00382-017-3796-5

Gettelman, A., Hannay, C., Bacmeister, J. T., Neale, R. B., Pendergrass, A. G., Danabasoglu, G., Lamarque, J.-F., Fasullo, J. T., Bailey, D. A., Lawrence, D. M., & Mills, M. J. (2019). High Climate Sensitivity in the Community Earth System Model Version 2 (CESM2). *Geophysical Research Letters*, *46*(14), 8329–8337. https://doi.org/10.1029/2019GL083978

Gettelman, A., & Morrison, H. (2015). Advanced Two-Moment Bulk Microphysics for Global Models. Part I: Off-Line Tests and Comparison with Other Schemes. *Journal of Climate*, *28*(3), 1268–1287. https://doi.org/10.1175/JCLI-D-14-00102.1

Gettelman, A., Morrison, H., Eidhammer, T., Thayer-Calder, K., Sun, J., Forbes, R., McGraw, Z., Zhu, J., Storelvmo, T., & Dennis, J. (2022). Importance of Ice Nucleation and Precipitation on Climate with the Parameterization of Unified Microphysics Across Scales version 1 (PUMASv1). *EGUsphere*, 1–28. https://doi.org/10.5194/egusphere-2022-980

Hoose, C., Kristjánsson, J. E., Chen, J.-P., & Hazra, A. (2010). A Classical-Theory-Based Parameterization of Heterogeneous Ice Nucleation by Mineral Dust, Soot, and Biological Particles in a Global Climate Model. *Journal of the Atmospheric Sciences*, *67*(8), 2483–2503. https://doi.org/10.1175/2010JAS3425.1

Jiang, J. H., Su, H., Zhai, C., Perun, V. S., Del Genio, A., Nazarenko, L. S., Donner, L. J., Horowitz, L., Seman, C., Cole, J., Gettelman, A., Ringer, M. A., Rotstayn, L., Jeffrey, S., Wu, T., Brient, F., Dufresne, J.-L., Kawai, H., Koshiro, T., … Stephens, G. L. (2012). Evaluation of cloud and water vapor simulations in CMIP5 climate models using NASA "A-Train" satellite observations. *Journal of Geophysical Research: Atmospheres*, *117*(D14). https://doi.org/10.1029/2011JD017237

Kanji, Z. A., Ladino, L. A., Wex, H., Boose, Y., Burkert-Kohn, M., Cziczo, D. J., & Krämer, M. (2017). Overview of Ice Nucleating Particles. *Meteorological Monographs*, *58*(1), 1.1-1.33. https://doi.org/10.1175/AMSMONOGRAPHS-D-16-0006.1

Komurcu, M., Storelvmo, T., Tan, I., Lohmann, U., Yun, Y., Penner, J. E., Wang, Y., Liu, X., & Takemura, T. (2014). Intercomparison of the cloud water phase among global climate models. *Journal of Geophysical Research: Atmospheres*, *119*(6), 3372–3400. https://doi.org/10.1002/2013JD021119

Korolev, A., McFarquhar, G., Field, P. R., Franklin, C., Lawson, P., Wang, Z., Williams, E., Abel, S. J., Axisa, D., Borrmann, S., Crosier, J., Fugal, J., Krämer, M., Lohmann, U., Schlenczek, O., Schnaiter, M., & Wendisch, M. (2017). Mixed-Phase Clouds: Progress and Challenges. *Meteorological Monographs*, *58*(1), 5.1-5.50. https://doi.org/10.1175/AMSMONOGRAPHS-D-17-0001.1

Loeb, N. G., Doelling, D. R., Wang, H., Su, W., Nguyen, C., Corbett, J. G., Liang, L., Mitrescu, C., Rose, F. G., & Kato, S. (2018). Clouds and the Earth's Radiant Energy System (CERES) Energy Balanced and Filled (EBAF) Top-of-Atmosphere (TOA) Edition-4.0 Data Product. *Journal of Climate*, *31*(2), 895–918. https://doi.org/10.1175/JCLI-D-17-0208.1

Lohmann, U., & Neubauer, D. (2018). The importance of mixed-phase and ice clouds for climate sensitivity in the global aerosol–climate model ECHAM6-HAM2. *Atmospheric Chemistry and Physics*, *18*(12), 8807–8828. https://doi.org/10.5194/acp-18-8807-2018

Meyers, M. P., DeMott, P. J., & Cotton, W. R. (1992). New Primary Ice-Nucleation Parameterizations in an Explicit Cloud Model. *Journal of Applied Meteorology and Climatology*, *31*(7), 708–721. https://doi.org/10.1175/1520-0450(1992)031<0708:NPINPI>2.0.CO;2

Mitchell, J. F. B., Senior, C. A., & Ingram, W. J. (1989). C02 and climate: A missing feedback? *Nature*, *341*(6238), Article 6238. https://doi.org/10.1038/341132a0

Murray, B. J., Carslaw, K. S., & Field, P. R. (2021). Opinion: Cloud-phase climate feedback and the importance of ice-nucleating particles. *Atmospheric Chemistry and Physics*, *21*(2), 665–679. https://doi.org/10.5194/acp-21-665-2021

Rossow, W. B., & Schiffer, R. A. (1999). Advances in Understanding Clouds from ISCCP. *Bulletin of the American Meteorological Society*, *80*(11), 2261–2288. https://doi.org/10.1175/1520-0477(1999)080<2261:AIUCFI>2.0.CO;2

Shaw, J., McGraw, Z., Bruno, O., Storelvmo, T., & Hofer, S. (2022). Using Satellite Observations to Evaluate Model Microphysical Representation of Arctic Mixed-Phase Clouds. *Geophysical Research Letters*, *49*(3), e2021GL096191. https://doi.org/10.1029/2021GL096191

Sherwood, S. C., Webb, M. J., Annan, J. D., Armour, K. C., Forster, P. M., Hargreaves, J. C., Hegerl, G., Klein, S. A., Marvel, K. D., Rohling, E. J., Watanabe, M., Andrews, T., Braconnot, P., Bretherton, C. S., Foster, G. L., Hausfather, Z., von der Heydt, A. S., Knutti, R., Mauritsen, T., … Zelinka, M. D. (2020). An Assessment of Earth's Climate Sensitivity Using Multiple Lines of Evidence. *Reviews of Geophysics*, *58*(4), e2019RG000678. https://doi.org/10.1029/2019RG000678

Sourdeval, O., Gryspeerdt, E., Krämer, M., Goren, T., Delanoë, J., Afchine, A., Hemmer, F., & Quaas, J. (2018). Ice crystal number concentration estimates from lidar–radar satellite remote sensing – Part 1: Method and evaluation. *Atmospheric Chemistry and Physics*, *18*(19), 14327–14350. https://doi.org/10.5194/acp-18-14327-2018

Storelvmo, T., & Tan, I. (2015). The Wegener-Bergeron-Findeisen process – Its discovery and vital importance for weather and climate. *Meteorologische Zeitschrift*, *24*(4), 455–461. https://doi.org/10.1127/metz/2015/0626

Storelvmo, T., Tan, I., & Korolev, A. V. (2015). Cloud Phase Changes Induced by CO2 Warming—A Powerful yet Poorly Constrained Cloud-Climate Feedback. *Current Climate Change Reports*, *1*(4), 288–296. https://doi.org/10.1007/s40641-015-0026-2

Tan, I., & Storelvmo, T. (2016). Sensitivity Study on the Influence of Cloud Microphysical Parameters on Mixed-Phase Cloud Thermodynamic Phase Partitioning in CAM5. *Journal of the Atmospheric Sciences*, *73*(2), 709–728. https://doi.org/10.1175/JAS-D-15-0152.1

Tan, I., Storelvmo, T., & Zelinka, M. D. (2016). Observational constraints on mixed-phase clouds imply higher climate sensitivity. *Science*, *352*(6282), 224–227. https://doi.org/10.1126/science.aad5300

Zelinka, M. D., Klein, S. A., & Hartmann, D. L. (2012). Computing and Partitioning Cloud Feedbacks Using Cloud Property Histograms. Part II: Attribution to Changes in Cloud Amount, Altitude, and Optical Depth. *Journal of Climate*, *25*(11), 3736–3754. https://doi.org/10.1175/JCLI-D-11-00249.1

Zelinka, M. D., Myers, T. A., McCoy, D. T., Po-Chedley, S., Caldwell, P. M., Ceppi, P., Klein, S. A., & Taylor, K. E. (2020). Causes of Higher Climate Sensitivity in CMIP6 Models. *Geophysical Research Letters*, *47*(1), e2019GL085782. https://doi.org/10.1029/2019GL085782

Zelinka, M. D., Zhou, C., & Klein, S. A. (2016). Insights from a refined decomposition of cloud feedbacks. *Geophysical Research Letters*, *43*(17), 9259–9269. https://doi.org/10.1002/2016GL069917

Zhu, J., Otto-Bliesner, B. L., Brady, E. C., Gettelman, A., Bacmeister, J. T., Neale, R. B., Poulsen, C. J., Shaw, J. K., McGraw, Z. S., & Kay, J. E. (2022). LGM Paleoclimate Constraints Inform Cloud Parameterizations and Equilibrium Climate Sensitivity in CESM2. *Journal of Advances in Modeling Earth Systems*, *14*(4), e2021MS002776. https://doi.org/10.1029/2021MS002776

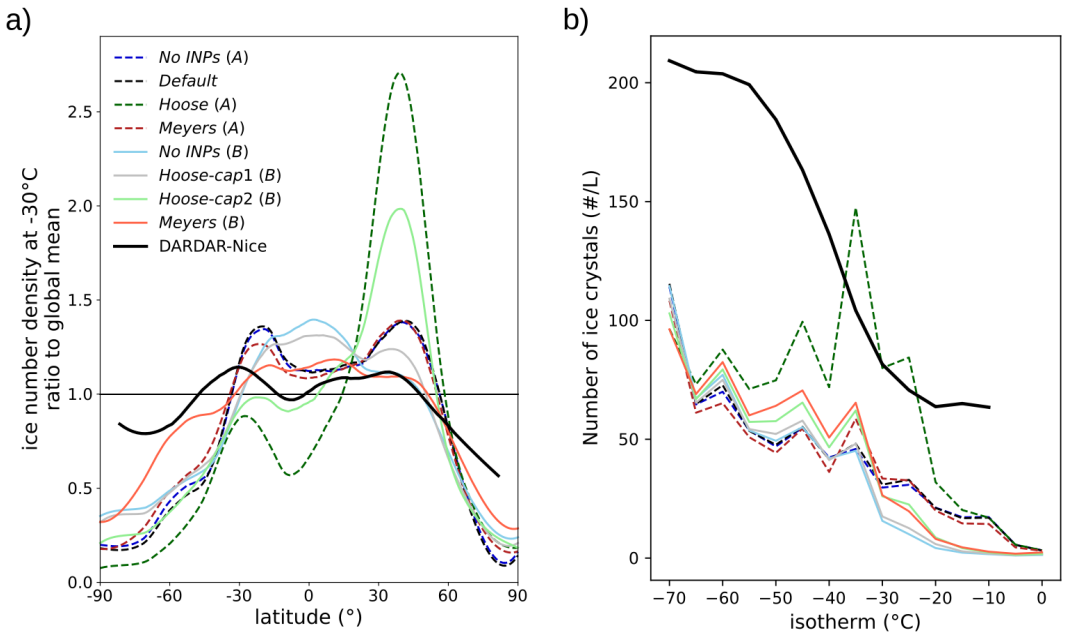

Figure S1 | Ice number density in present-day simulations and DARDAR-Nice satellite retrievals, showing spatial variability of in-cloud ice crystal number near -30°C **(a)** and global mean values across isotherms **(b)**. Data in (a) is normalized by each simulation's global mean value to emphasize differences in spatial structure. This data includes only ice crystals >5μm diameter within ±1°C of each isotherm with gaps of 5°C. To reduce noise in (a), polynomial smoothing was applied using a window of 20° latitude.

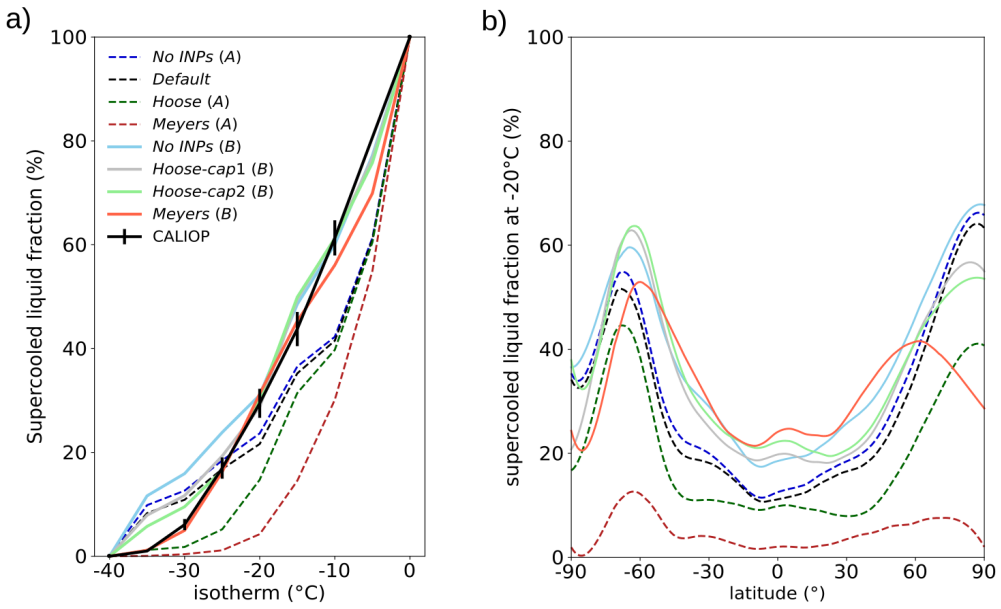

Figure S2 | Supercooled liquid fraction in present-day simulations and CALIOP retrievals, shown by isotherm **(a)** and also by latitude for the -20°C isotherm **(b)**. Only clouds visible to CALIOP are shown, such that clouds under optically thick cloud layers (optical depth τ>3) are ignored. Global mean values are in Table 1. As in Fig. S1a, polynomial smoothing was applied to (b) using a window of 20° latitude.

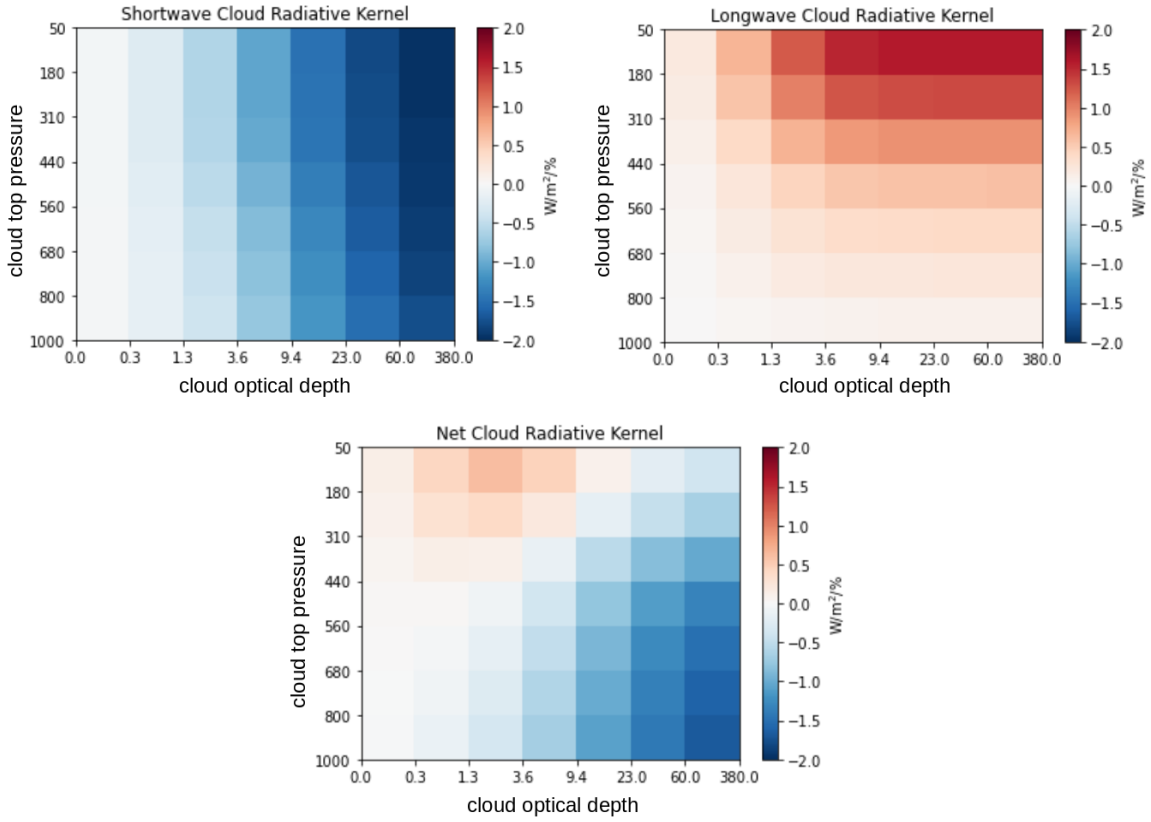

Figure S3 | Radiative kernels used in this study, showing impacts of % changes of each cloud type on shortwave (SW), longwave (LW), and net (SW+LW) radiation. This is as in Fig. 1 of Zelinka et al. (2012a), but here SW influence is averaged over surface albedo data from default CESM2.

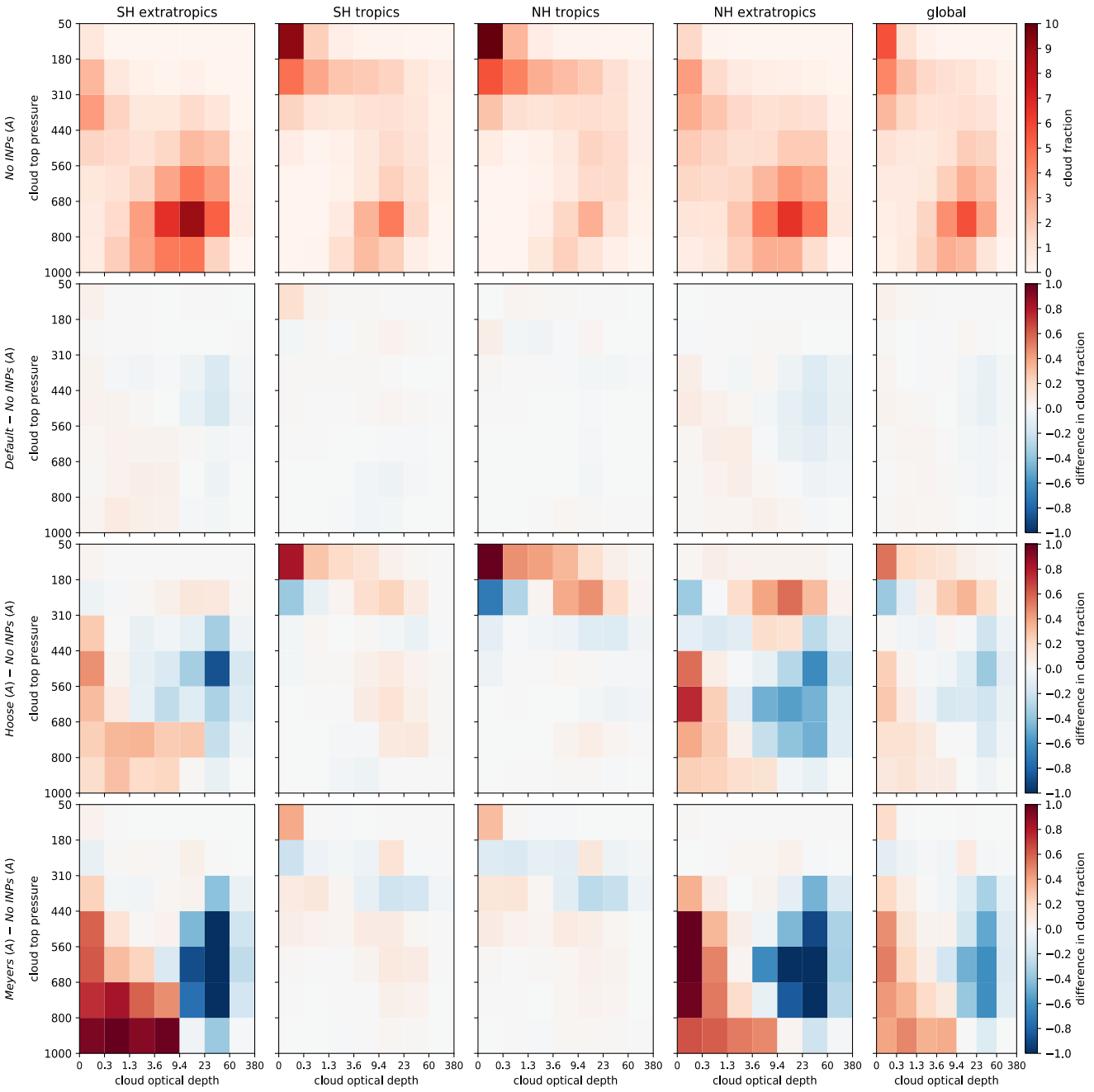

Figure S4 | Cloud types identified in ISCCP cloud histograms, showing changes to prevalence of 49 cloud types. Cloud types are separated by cloud top pressure and optical depth and are shown as standard output for comparison with ISCCP. Output from *No INPs (A)* is shown directly, while the other unadjusted experiments are shown as difference from these cases for clarity. Note that the difference plots have a color bar ten times stronger than those for *No INPs (A)*. Group B experiments are shown separately in Fig. S5.

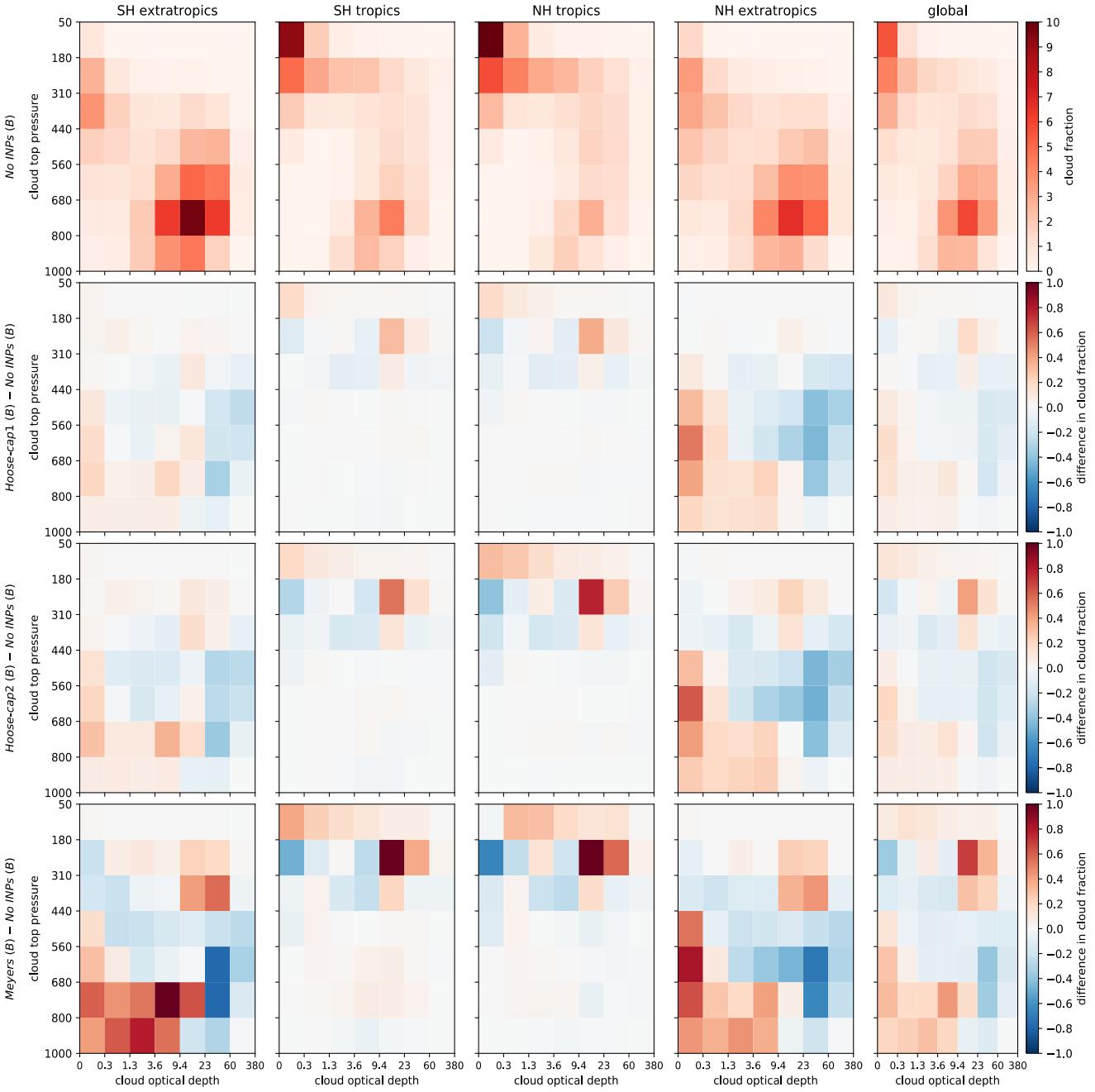

Figure S5 | as in Figure S4 but among the Group B simulations, with experiments here compared to *No INPs (B)*.

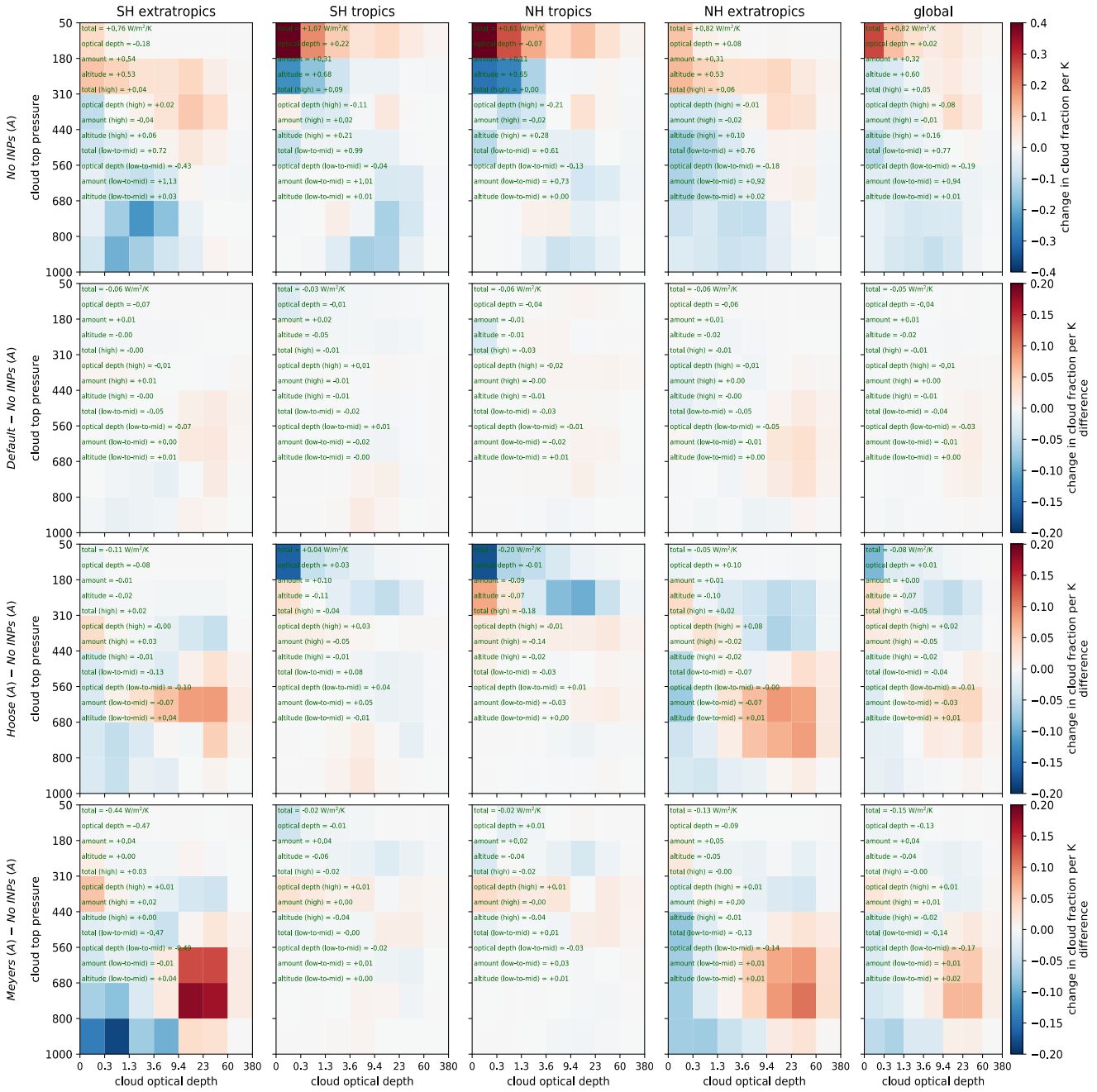

Figure S6 | Cloud changes as warming occurs as identified in ISCCP cloud histograms. Aside for the top row (*No INPs (A, SST+4K) – No INPs (B, present-day)*), the data is shown as four-way differences, i.e. (*experiment*(A, SST+4K) – *experiment(A, present-day)*) – (*No INPs (B, SST+4K) – No INPs (B, present-day)*). Also included on the plots in green text are cloud feedbacks calculated by the kernel method (showing feedback differences compared to *No INPs (A)* below the first row), with low and mid-level clouds grouped together to conserve space. Note that the four-way difference plots have a colorbar twice as strong as the top row. For differences in present-day clouds among the same simulations, see Fig. S4.

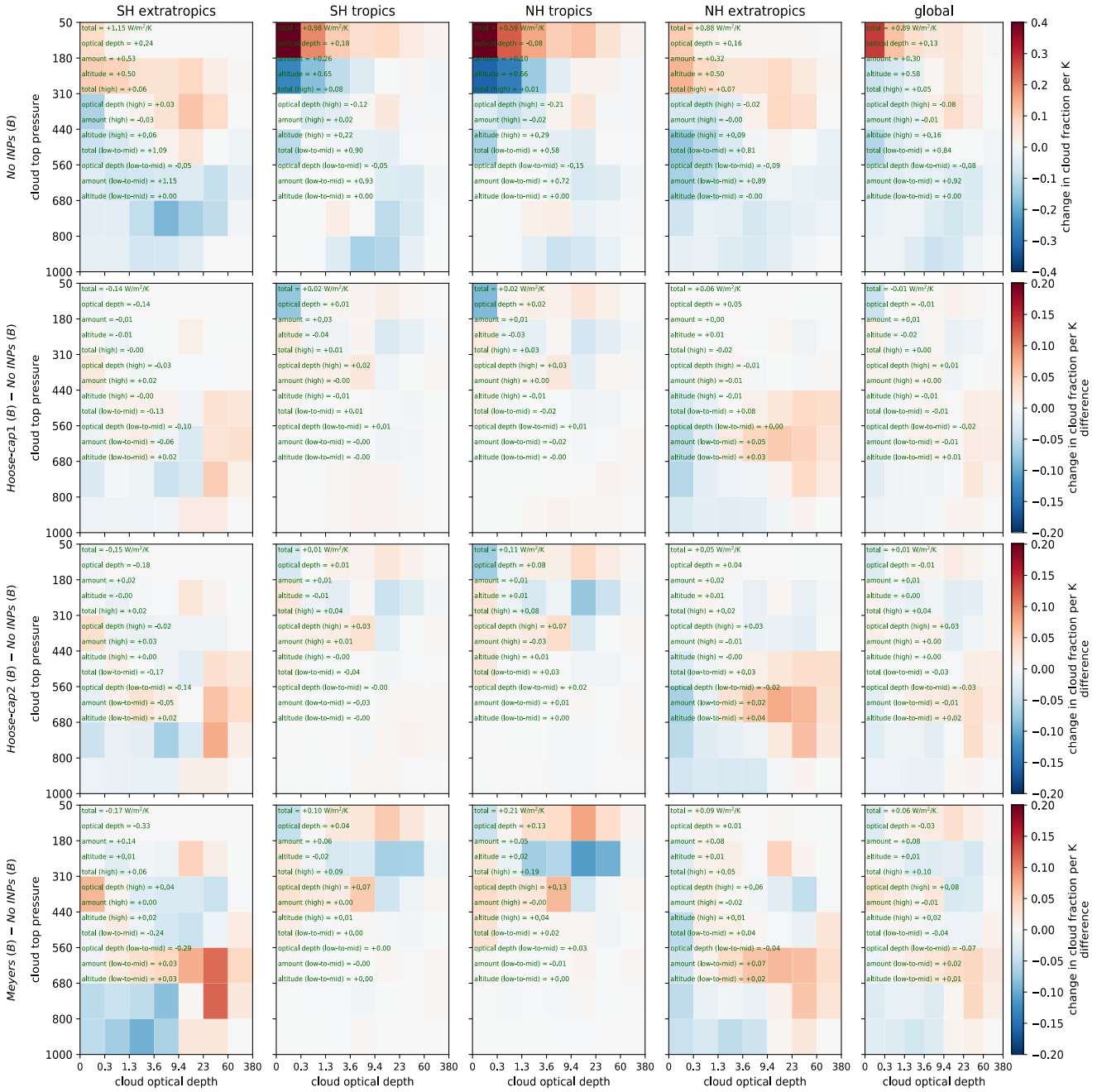

Figure S7 | as in Figure S6 but among the Group B simulations, with experiments being compared to *No INPs (B)*. For differences in present-day clouds among the same experiments, see Fig. S5.

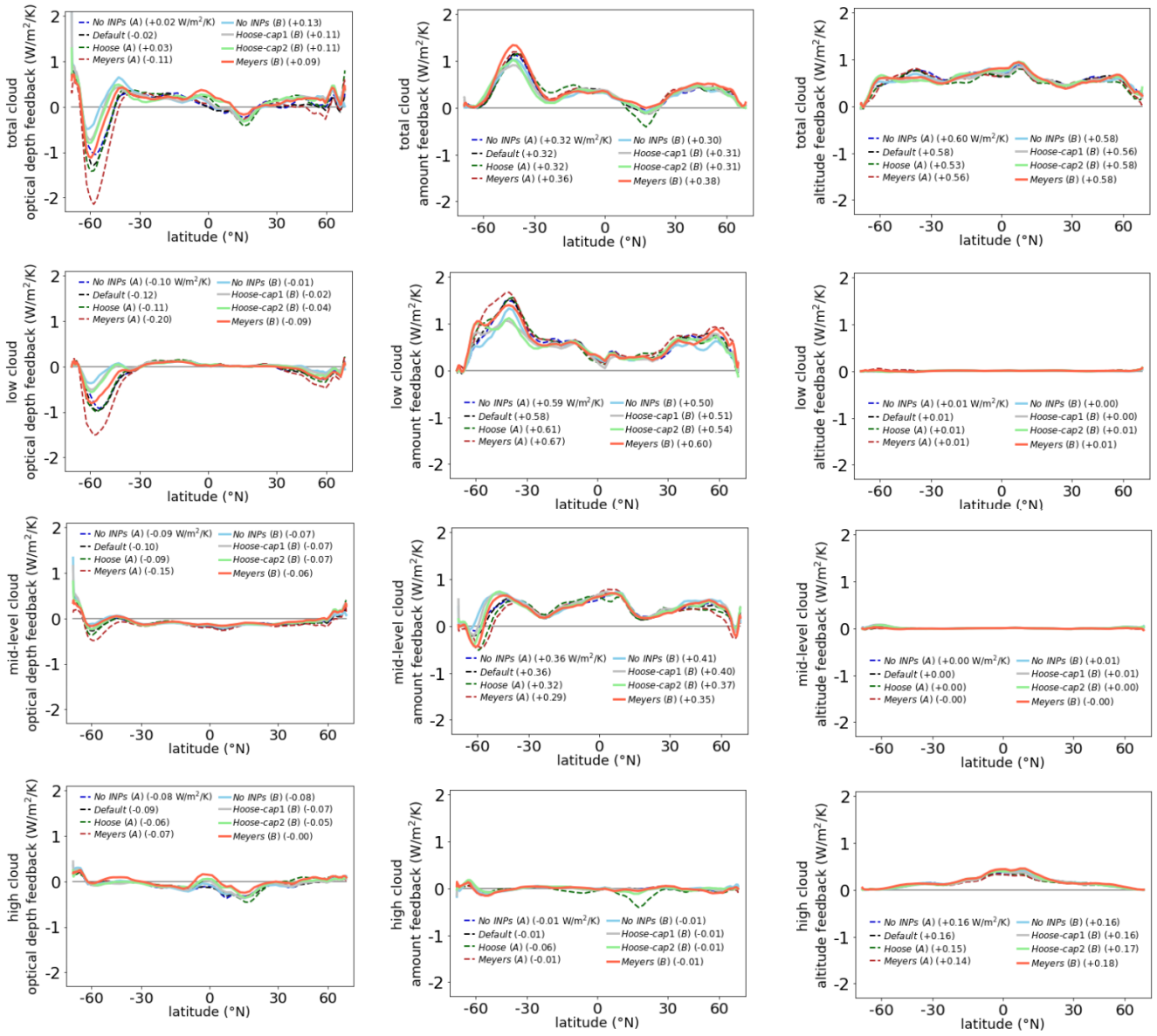

Figure S8 | Cloud feedbacks separated by mechanism in all CESM2 simulations, as in Fig. 3b but further partitioned by mechanism. Global mean feedback values are included in each legend. Note that some mismatch exists between the sum of feedbacks between levels and each unseparated feedback (Zelinka et al., 2016), shown here in the top row.